Perennial pack ice in the southern Beaufort Sea was not as it appeared in the summer of 2009

David G. Barber,[1] Ryan Galley,[1] Matthew G. Asplin,[1] Roger De Abreu,[4] Kerri-Ann Warner,[1] Monika Pućko,[1,2] Mukesh Gupta,[1] Simon Prinsenberg,[3] and Stéphane Julien[5]

Received 22 October 2009; revised 13 November 2009; accepted 23 November 2009; published 24 December 2009.

[1] In September 2009 we observed a much different sea icescape in the Southern Beaufort Sea than anticipated, based on remotely sensed products. Radarsat derived ice charts predicted 7 to 9 tenths multi-year (MY) or thick first-year (FY) sea ice throughout most of the Southern Beaufort Sea in the deep water of the Canada Basin. *In situ* observations found heavily decayed, very small remnant MY and FY floes interspersed with new ice between floes, in melt ponds, thaw holes and growing over negative freeboard older ice. This icescape contained approximately 25% open water, predominantly distributed in between floes or in thaw holes connected to the ocean below. Although this rotten ice regime was quite different that the expected MY regime in terms of ice volume and strength, their near-surface physical properties were found to be sufficiently alike that their radiometric and scattering characteristics were almost identical. **Citation:** Barber, D. G., R. Galley, M. G. Asplin, R. De Abreu, K.-A. Warner, M. Pućko, M. Gupta, S. Prinsenberg, and S. Julien (2009), Perennial pack ice in the southern Beaufort Sea was not as it appeared in the summer of 2009, *Geophys. Res. Lett.*, *36*, L24501, doi:10.1029/2009GL041434.

1. Introduction

[2] Observed changes in annual sea ice extent and thickness in the northern hemisphere are commensurate with increasing regional temperatures, increased mass fluxes from northern hemisphere glaciers, increasing permafrost temperature, increasing air temperature and increasing ocean mixed layer depth temperatures in summer [*Intergovernmental Panel on Climate Change*, 2007]. An average decrease in the extent of sea ice in September of about 45,100 kmP^{2}/year (±4600 kmP^{2}), coincident with a decrease in the winter sea ice extent of 39,500 kmP^{2}/year (±5600 kmP^{2}) between 1979 and 2006 has been recorded using passive microwave remote sensing [*Parkinson and Cavalieri*, 2008]. Northern hemisphere sea ice thickness has also decreased in the past half century, by up to 40% in some regions [*Rothrock et al.*, 1999; *Hilmer and Lemke*, 2000]. The consequences of this transformation from a multi-year (MY) sea ice cover to one dominated by seasonal sea ice has implications throughout the Arctic marine, terrestrial and freshwater ecosystems. These changes also impact indigenous populations who rely upon the ice cover for subsistence hunting, resource exploration and development projects, and the security and sovereignty of northern waterways due to the ease of sailing through younger, thinner ice.

[3] Sea ice information for ship operations in ice and research purposes are gleaned primarily from active and/or passive microwave satellite remote sensing. Here, we present *in situ* sea ice conditions that were different in the southern Beaufort Sea than conditions inferred from active and passive microwave remote sensing. We present *in situ* physical observations of a predominately first-year (FY) sea ice cover in the southeastern Beaufort Sea where high concentrations of MY or thick FY sea ice were inferred remotely, and discuss why this thin ice was mistaken for the thicker FY and MY types. This case of mistaken identity brings to light the difficulty in correctly characterizing variable ice covers remotely in fall when many different ice types are present simultaneously. It also highlights the fact that sea ice thought to be thick, end-of-the-year FY or MY, can in fact be very thin, and could have large climate [e.g., *Perovich et al.*, 2008] and marine navigation implications [*De Abreu et al.*, 2003].

2. Methods

[4] *In situ* observations of the atmosphere-sea ice-ocean system in the southeastern Beaufort Sea were made from the Canadian Research Icebreaker (NGCC) *Amundsen* deployed for the ArcticNet/IPY−GeoTraces project between 27 August and 12 September 2009. The cruise track is shown in Figure 1. Canadian Ice Service (CIS) digital ice charts were employed for real-time planning of station locations and sailing routes during the cruise. CIS digital ice charts are based on expert manual interpretation of Radarsat-1 data (the primary data source since 1996), NOAA-AVHRR and Envisat Advanced Synthetic Aperture Radar (ASAR) data and *in situ* aerial and marine surveys. They include total sea ice concentration and partial concentrations by type. We present information collected at stations L1, L1.5, L2 and MYI (Figure 1).

[5] A conductivity-temperature-depth (CTD) profile of the near-surface ocean column was made from the ship's zodiac using an Idronaut Ocean Seven model 304 CTD. MY ice was physically sampled at station L1 on 31 August 2009, and heavily decayed first-year (FY) ice (rotten ice) at station L2 on 4 September 2009 (Figure 1). Sea ice temperature profiles were measured immediately after extracting the ice core (using a Kovacs Mark II coring system) by placing a temperature probe in holes drilled at 10 cm intervals beginning

[1]Centre for Earth Observation Science, Faculty of Environment, Earth and Resources, University of Manitoba, Winnipeg, Manitoba, Canada.
[2]Freshwater Institute, Fisheries and Oceans, Winnipeg, Manitoba, Canada.
[3]Bedford Institute of Oceanography, Fisheries and Oceans, Halifax, Nova Scotia, Canada.
[4]Canadian Ice Service, Environment Canada, Ottawa, Ontario, Canada.
[5]Laurentian Region, Canadian Coast Guard, Quebec, Quebec, Canada.

0094-8276/09/2009GL041434$05.00

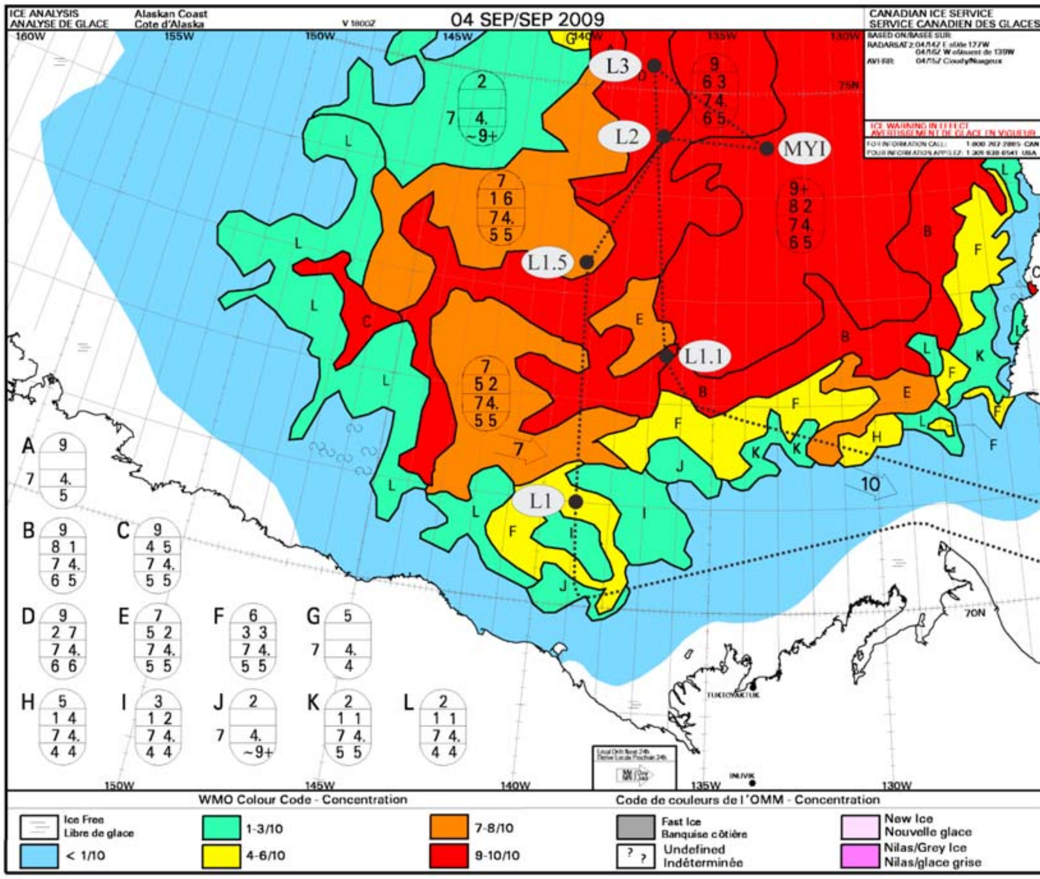

Figure 1. Study area showing the transit of the *Amundsen* on the ArcticNet/IPY-Geotraces project, 27 August to 12 September 2009 overlaid on a CIS ice chart for 4 September 2009.

at 5 cm. Sea ice salinity was measured by cutting a second core into 10 cm sections, placing them in sealed buckets and melting them. Salinity of the melt was calculated from conductivity and temperature using a HACH SENSION5 portable conductivity meter (±0.01 psu). Sea ice thickness was measured *in situ* with a measuring tape. Meteorological variables were monitored with an AXYS Automated Voluntary Observation System (AVOS) mounted above the ship's wheelhouse. Cloud fractional cover and type were recorded manually every three hours, and cloud heights were monitored continuously using a Vaisala ceilometer. Downwelling longwave (L↓) and shortwave radiation (K↓) were collected using an Eppley PIP pyrgeometer and PSP pyranometer.

[6] Extensive sea ice thickness surveys were made at stations L2 and MYI (Figure 1) using a helicopter-mounted electromagnetic (EM) induction system called IcePic, including a laser altimeter, GPS and a nadir-facing video system. The near-circular footprint of the IcePic system is roughly 2.5 times the altitude (~2–4 m) at which it is flown.

[7] A surface-based polarimetric C-band scatterometer (similar to Radarsat-1's SAR) was used to make *in situ* measurements of active microwave scattering from the port side of the *Amundsen* (~8 m from the surface). Each scan was executed with the following parameters: azimuth: 0° to 60°, and elevation 20° to 60°, which was measured in 5° increments. Similarly, a surface-based radiometer (SBR) monitored passive microwave emissions at 37 and 89 GHz on the port side (~10 m from the surface); brightness temperatures were recorded at elevation angles between 30°–70° for vertical (V) and horizontal (H) polarizations.

3. Results and Discussion

[8] Surface meteorological conditions measured in the vicinity of the *Amundsen* during the cruise show a cloudy, nearly isothermal surface environment, with low stratus cloud cover (<150 m) and fog recurrent throughout the cruise. Air temperatures ranged from −5.6°C to +1.2°C (mean = −1.4°C). Relative humidity was 81–99% (mean = 92%), and cloud-fractional cover ranged from 750–100%. Maximum values of down-welling shortwave observed during the cruise ranged from 70–170 W mP^{2}, depending on cloud cover. Values of down-welling longwave ranged from 307–313 W mP^{2} illustrating the important role of the longwave flux to surface warming.

[9] We departed from station L1 (Figure 1) heading north towards station L1.5, expecting to enter MY sea ice cover at about 71°20′N, 139°00′W based on remotely sensed information (Orange polygon in Figure 1). The CIS ice chart (which relies extensively on Radarsat-1 data) for 4 September 2009 indicated the ship track would range from 7 to 9 tenths coverage and this ice would consist of partial concentrations of 5 tenths to 7 tenths old ice and from 2 to 3 tenths thick first year ice (see egg codes in Figure 1); details on reading the egg codes can be found at http://www.ice-glaces.ec.gc.ca.

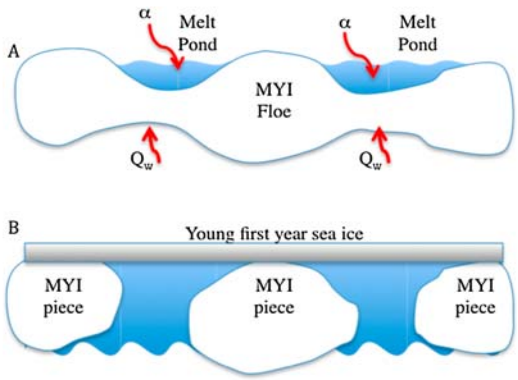

Figure 2. Conceptual schematic of the rotten ice encountered along the transect line from just north of station L1, through station L1.5 to station L2 (Figure 1). The small remnant pieces of thick FY, second year and MY sea ice were sufficiently decayed that melt ponds thawed through to melt holes and many of these pieces had negative freeboard. These remnant pieces then were overgrown with new ice (~5 cm thick).

[10] *In situ* observations of the sea ice conditions however showed that the ice we were traversing was not MY or thick FY, nor was it 7 to 9 tenths concentration, but rather it was a mixture of a few small MY ice floes (1 tenth coverage) interspersed in a cover dominated by small (10–100 m) rounded floes of heavily decayed first year sea ice (4 tenths). These floes were overlain by a thin layer of new ice (7 tenth) where freeboard was negative and thin ice growing between remnant pieces when the ice had a positive freeboard (Figure 2). Likewise, some new ice covered open water areas between floes. These rotten first year floes were likely the result of melt ponds thawing completely through a larger floe and subsequent survival of the thicker drained piece due to it's relatively higher albedo. These small floes formed a somewhat stable surface which decreased wind roughening of the surface, permitting new sea ice to form over thaw holes and in open areas between these rotten floe pieces (Figure 2). The new ice on top was about 5 cm thick, indicating it has just recently begun to grow.

[11] The salinity and temperature of rotten ice at station L2 on 4 September 2009 (Figure 3) were indicative of very late season sea ice. The rotten ice salinity was below about 3 psu in the middle, decreasing towards the surface and bottom due to drainage of the volume during the melt season (Figure 3). The rotten ice was 1.27 m thick. MY ice salinity was very similar with 0 at the surface to 3.5 psu in the middle of the volume (thickness = 4.00 m). In both cases, the sea ice was nearly isothermal (Figure 3). This low salinity and high internal temperature resulted in highly weakened ice [*Timco and Johnston*, 2002].

[12] Beneath the sea ice on 5 September 2009 a CTD profile indicated that the surface mixed layer was cooling (Figure 3: bottom) which makes sense in the context of the new ice formation observed at the surface throughout the study area. Throughout the length of our south to north transect (stations L1 through L1.5 to L2; Figure 1) the *Amundsen* was able to sail at an average speed of 24 km·hP^{-1} (13 nm·hP$^{-1)}$). The *Amundsen*'s open water cruising speed is about 25 km·hP^{-1} (13.7 nm·hP^{-1}).

[13] An extensive (~40 km) EM ice thickness flight was conducted in the vicinity of station L2 (4 September 2009) that characterized the ice thickness distribution of the region (Figure 4). The mean (median) ice thickness was 0.57 m (0.44 m) in an area dominated by heavily decayed FY sea ice. The percent of sea ice in this area greater than 1.00 m (2.00 m) was 14.1% (3.3%). Between stations L2 and MYI (Figure 1) we progressed through very heavily decayed thin and heavily rotted FY ice into a region of less decayed FY sea ice, and finally into MY pack ice. The transition to the MY pack occurred around 134 W, and not as indicated in the ice chart,

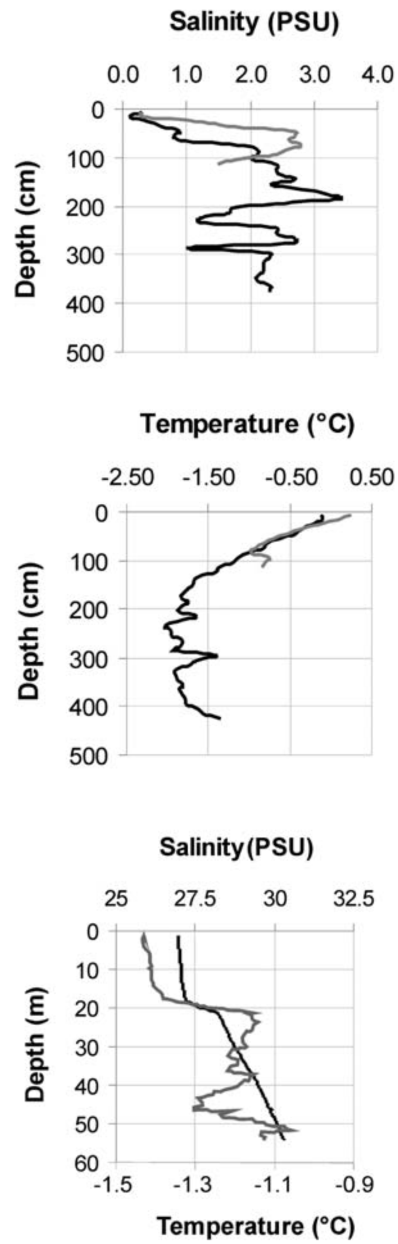

Figure 3. Profiles of (top) salinity and (middle) temperature in MY (black) and rotten FY ice (grey), 31 August 2009 at station L1 and 4 September 2009, at station L2 respectively. Ocean profile (bottom) showing salinity (black) and temperature (grey, °C) in the top 50 m of the ocean, 5 September 2009.

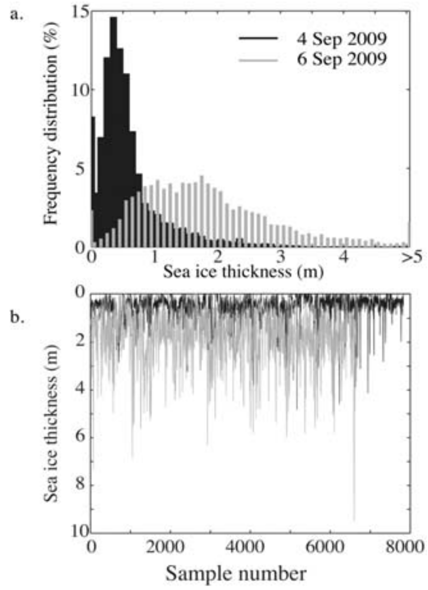

Figure 4. Examples of the (a) thickness and (b) surface roughness of the rotten FY ice (4 September 2009) and thick MY ice at the MYI station (6 September 2009) sampled with the helicopter mounted Electromagnetic Induction (EMI) system.

at about 136 W (along the transect line between L2 and MYI; Figure 1).

[14] We found the thick MY (Figure 1, station MYI) ice was also heavily decayed; the *Amundsen* was able to break through thick floes (6–8 m thick) making way at about 9.3 $km \cdot hP^{-1} \pm 5$ $nm \cdot hP^{-1}$). The CIS digital ice chart for 4 September 2009 (Figure 1) showed that station MYI was located in 9+ tenths sea ice, 8 tenths of which was old ice and 2 tenths thick FY ice. Station MYI was found to be a much different sea ice regime than station L2 using the helicopter mounted EM thickness system (Figure 3 in grey). The mean (median) thickness in this area over ~35 km of surveys on 6 September 2009 was 1.83 m (1.65 m). The percent of sea ice in the vicinity of the MYI station greater than 1.00 m (2.00 m) was 75.8% (36.0%) indicating a substantial shift toward thicker (older) sea ice from station L2 to MYI (Figure 3).

[15] These two very different icescapes had very similar microwave scattering and emission characteristics, thus making it difficult to differentiate them electromagnetically. We found an average scattering to our *in situ* scatterometer of −15dB for both MY and rotten ice types at 35° incidence. Similarly radiometer data (37 and 89 GHz) show a similar overlap in the brightness temperatures (e.g., 218 K ± 3 K at 50° incidence at 89 V). Further analysis of the electromagnetic characteristics of these overlapping ice classes is being prepared (D. G. Barber et al., Active and passive microwave remote sensing of late season rotten and multiyear sea ice in the Southern Beaufort Sea, manuscript in preparation, 2009). Physically, both rotten/thin FY and MY ice types sampled were close to isothermal and had very similar near-surface temperature profiles and similar and low near-surface salinity (Figure 3). Further, both types/areas had similar open water and new sea ice fractions at the surface (Figure 3). This resulted in volume scattering and emission being the principal scattering mechanism making it difficult to differentiate these very different ice regimes.

4. Conclusions

[16] In situ observations from NGCC *Amundsen* indicate that the MY sea icescape in the southern Beaufort Sea was not as ubiquitous as it appeared in satellite remote sensing (Figure 1) in early September 2009. A large sector of what was remotely sensed to be MY sea ice at 7 to 9 tenths ice cover, consisting primarily of large to vast MY ice floes, was in fact a surface of heavily decayed ice composed of some small MY floes (1 tenth) interspersed in a cover dominated by heavily decayed FY floes (4 tenths) and overlain by new sea ice in areas of negative freeboard and in open water between floes. In some areas (e.g., stations L1 and MYI: Figure 1) the ocean surface was dominated in some areas by MY sea ice that was much thicker than the heavily decayed FY sea ice previously discussed. This case of mistaken identity is physically explained by the factors which contribute to the return to Radarsat-1 from the two surfaces; both ice regimes had similar temperature and salinity profiles in the near-surface volume, both ice types existed with a similar amount of open water between and within the floes, and finally both ice regimes were overlain by similar, recently formed new sea ice in areas of negative freeboard and in open water areas. The fact that these two very different ice regimes could not be differentiated using Radarsat-1 data or *in situ* C-band scatterometer or microwave radiometer measurements, has significant implications for climate studies and for marine vessel navigation in the Canada Basin. The results also suggest that operational agencies (such as the CIS) should consider making ice decay a variable in their ice charts. The presence of this rotten ice regime in the centre and western limit of the Beaufort pack ice allows for wind generated swells to penetrate far into the last remaining MY ice along the Canadian Archipelago further weakening the continuity of the MY pack (M. Asplin, Dynamic and thermodynamic implications of storm swell induced fracturing of the summer perennial pack ice in the southern Beaufort Sea, manuscript in preparation, 2009). Our results are consistent with ice age estimates (Fowler and Maslanik, http://nsidc.org/news/press/20091005_minimumpr.html) that show the amount of MY sea ice in the northern hemisphere was the lowest on record in 2009 suggesting that MY sea ice continues to diminish rapidly in the Canada Basin even though 2009 areal extent increased over that of 2007 and 2008.

[17] **Acknowledgments.** This work would not have been possible without the expertise of the crew of the NGCC *Amundsen*, and data support from the Canadian Ice Service. Thanks to ArcticNet, the Canada Research Chairs program, the International Polar Year Federal Program Office, and NSERC for funding.

References

De Abreu, R. A., J. U. Yackel, D. Barber, and M. Arkett (2003), Operational satellite sensing of Arctic first year sea ice melt, *Can. J. Remote Sens.*, *24*, 487–501.

Hilmer, M., and P. Lemke (2000), On the decrease of Arctic sea ice volume, *Geophys. Res. Lett.*, *27*, 3751–3754, doi:10.1029/2000GL011403.

Intergovernmental Panel on Climate Change (2007), *Climate Change 2007: The Physical Science Basis: Contribution of Working Group I to the Fourth Assessment Report of the Intergovernmental Panel on Climate Change*, edited by S. Solomon et al., Cambridge Univ. Press, New York.

Parkinson, C. L., and D. J. Cavalieri (2008), Arctic sea ice variability and trends, 1979–2006, *J. Geophys. Res.*, *113*, C07003, doi:10.1029/2007JC004558.

Perovich, D. K., J. A. Richter-Menge, K. F. Jones, and B. Light (2008), Sunlight, water, and ice: Extreme Arctic sea ice melt during the summer of 2007, *Geophys. Res. Lett.*, *35*, L11501, doi:10.1029/2008GL034007.

Rothrock, D. A., Y. Yu, and G. A. Maykut (1999), Thinning of the Arctic sea-ice cover, *Geophys. Res. Lett.*, *26*, 3469–3472, doi:10.1029/1999GL010863.

Timco, G. W., and M. E. Johnston (2002), Sea ice strength during the melt season, paper presented at the 16th LAHR International Symposium on Ice, Univ. of Otago, Dunedin, New Zealand, 2–6 Dec.

M. G. Asplin, D. G. Barber, R. Galley, M. Gupta, M. Pućko, and K.-A. Warner, Centre for Earth Observation Science, Faculty of Environment, Earth and Resources, University of Manitoba, 476 Wallace Bldg., Winnipeg, MB R3T 2N2, Canada. (dbarber@cc.umanitoba.ca)

R. De Abreu, Canadian Ice Service, Environment Canada, 373 Sussex Dr., Ottawa, ON K1A 0H3, Canada.

S. Julien, Laurentian Region, Canadian Coast Guard, 101, blvd. Champlain, Quebec, QC G1K 7Y7, Canada.

S. Prinsenberg, Bedford Institute of Oceanography, Fisheries and Oceans, PO Box 1006,1 Challenger Dr., Sta. B220, Halifax, NS B2Y 4A2, Canada.